Mobile Ranging Using Low-Accuracy Clocks

Dennis D. McCrady, *Senior Member, IEEE*, Lawrence Doyle, Howard Forstrom, Timothy Dempsey, and Marc Martorana

***Abstract*—Our position-location technique provides location information within milliseconds and is integrated in a handheld direct-sequence spread-spectrum (DSSS) communications system. We use a standard DSSS waveform, with a state-of-the-art chipping rate to provide a position location capability to an accuracy of less than 1 m in a severe multipath environment. We use a two-way time-of-arrival (TOA) measurement technique with 1-ppm clocks that eliminates the need to synchronize master and reference radio clocks. Several techniques improve TOA and, therefore, range accuracy. A loop back calibrates internal system delay. Frequency diversity orthogonalizes multipath with respect to direct path, and leading edge curve fitting of the direct path reduces the effect of multipath. Applications include location of urban war fighters, firefighters, police, and medical personnel and resources.**

***Index Terms*—Distance measurements, position measurement, source location.**

I. Introduction

THE capability to rapidly and accurately determine the physical location of a mobile communication device is of great benefit in a variety of applications. In a military context, it is desirable to know the location of military personnel and/or equipment during coordination of field operations and rescue missions. This includes scenarios where signals of conventional position-determining systems, such as the global positioning system (GPS), may not be available, e.g., within a building. More generally, appropriately equipped mobile communication devices can be used to track the position of personnel and resources located both indoors and outdoors. This includes, but is not limited to, police engaged in tactical operations, firefighters located near or within a burning building, medical personnel and equipment in a medical facility or en route to an emergency scene (including doctors, nurses, paramedics and ambulances), and personnel involved in search and rescue operations. An integrated position location communication device will also allow high-value items to be tracked and located, including such items as personal computers, laptop computers, portable electronic devices, luggage, briefcases, valuable inventory, and stolen automobiles. In urban environments, where conventional position determining systems have more difficulty operating, it would be desirable to reliably track fleets of commercial or industrial vehicles, including trucks, buses, and rental vehicles. Tracking of people carrying a mobile communication device is also desirable in a number of contexts, including, but not limited to, children in a crowded environment (such as a mall, amusement park or tourist attraction), location of personnel within a building, and location of prisoners in a detention facility.

The capability to determine the position of a mobile communication device also has application in locating the position of cellular telephones. Unlike conventional land-based/wire-connected telephones, the location of conventional cellular telephones cannot automatically be determined by emergency response systems (e.g., the 911 system in the U.S.) when an emergency call is placed. Thus, assistance cannot be provided if the caller is unable to speak to communicate his or her location (e.g., when the caller is unconscious, choking, or detained against will). The capability to determine the position of cellular telephones can be used to pinpoint the location from which an emergency call has been made. Such information can also be used to assist in cell network management.

Naturally, in cases where a mobile communication device is being used primarily to transmit or receive voice, data, or video information, it is desirable to incorporate position location capabilities such that the device can communicate and establish position location without disruption of the voice, data, or video communication.

A conventional technique used to determine the position of a mobile communication device involves reception of timing signals transmitted from multiple transmitters at different, known locations, e.g., GPS satellites or ground-based transmitters [1]. The range to each transmitter is determined from the arrival time of the timing signals and the mobile communication device then computes its position using triangulation.

The accuracy and operability of such position location techniques can be severely degraded in the presence of multipath interference. Unfortunately, multipath interference can be severe in environments in which position location techniques have their greatest usefulness, such as in urban environments and/or inside buildings [2], since artificial structures create opportunities for signals to be reflected, thereby causing signals to arrive at the receiver via a number of different paths.

Attempts have been made in position location systems to mitigate the effects of multipath interference using one- [3], [4] and two-way nonreciprocal [5] time-of-arrival (TOA) and time-difference-of-arrival (TDOA) measurement systems. One-way systems determine the range between the mobile target and each fixed reference radio by measuring the one-way duration of time required for a signal to travel between the radios. This information can be determined from a one-way communication only if the target and reference radios remain synchronized to the same time reference. That is, the transmitting radio establishes the time of transmission of the signal based on its local clock. The receiving radio determines the TOA of the signal based on

Manuscript received October 11, 1999. This work was supported by the ITT A/CD IR&D Program.

The authors are with the Aerospace/Communications Division, ITT Industries, Clifton, NJ 07014-1993 USA.

Publisher Item Identifier S 0018-9480(00)05033-X.

its local clock that must constantly be synchronized to the same reference as the clock of the transmitter. The signal propagation duration can then be determined essentially by subtracting the time of transmission from the TOA. This is true for each reference radio that is required for the total location solution. In addition, the precise time synchronization required to accurately measure the duration of the signal propagation cannot tolerate significant time drift of any local clocks over time. Consequently, all of the clocks of the system must be highly accurate, thereby increasing the cost of the system.

The two-way-system example referenced above is an indoor system and requires an infrastructure of antennas and cells in the building that feed a central transmit/receive processor. Items being tracked contain a credit-card-sized transponder. A particular cell controller cycles among antennas determining distances to those in range of the transponder, using at least three antennas for the solution. By using a transponder technique, the electronics are simplified at the tracked item leading to an achievable bandwidth of 40 MHz because the processing is performed in the central processor. They are able to operate at ranges up to 30 m from their transponders.

Accordingly, there remains a need for a commercially viable reciprocal position location system capable of quickly and accurately determining the three-dimensional indoor or outdoor position of a compact mobile communication device in the presence of severe multipath interference. The novelty of the approach described herein is twofold. First, it is a two-way reciprocal technique, meaning each handheld unit in the network can use the other handheld units in the network as references in determining its location, i.e., a central basestation and associated infrastructure are not required. Secondly, our system uses frequency diversity to orthogonalize multipath with respect to direct path, which, combined with leading-edge curve fitting of the direct path, reduces the deleterious effect of multipath.

The following sections describe our two-way reciprocal ranging system that can be integrated within a handheld communication system for use in the aforementioned practical applications, and its expected performance.

II. System Description

A. General Ranging Technique

A mobile master radio uses a minimum of three mobile reference radios to determine location in three dimensions. TOA's determine the range to each reference radio and trilateration determines the location of the master radio with respect to the references. Multiple message exchanges between the master and reference radios determine the TOA's. The number of multiple trials (M) to each reference radio varies depending on the severity of the multipath. The protocol used for ranging is derived from the carrier sense multiple access-collision avoidance (CSMA-CA) protocol by converting the request-to-send (RTS) into the RTS-time-of-arrival (RTS-T) and by converting the clear-to-send (CTS) into the TOA message packet.

B. Detailed Ranging Technique and Waveform

Our spread-spectrum radio processes the acquisition sequence to provide time synchronization for the modem. For ranging, we use additional processing to refine the time synchronization estimate using the TOA synchronization sequence shown in Fig. 1. The nominal chipping rate is 32 MHz with quasi-band limited (QBL) shaping on each chip. The rate of the data portion of the RTS-T and TOA Message is 250 kb/s. The carrier frequency can be anywhere in our radio band.

RTS-T

TRANSEC			
Comm Acquisition	TOA Synchronization	Destination Address	Other Data
16 x 4 us symbols with 128 chips each	4096 chips 128 µs	16 bits 64 µs	16 bits 64 µs

TOA MESSAGE

TRANSEC					
Comm Acquisition	TOA Synchronization	Delay Calibration	Destination Address	Ranging Message	CRC
16 x 4 us symbols with 128 chips each	4096 chips 128 µs	16 bits 64 µs	16 bits 64 µs	184 bits 736 µs	32 bits 128 µs

TOA-S MESSAGE

TRANSEC			
Comm Acquisition	TOA Synchronization	Destination Address	Other Data
16 x 4 us symbols with 128 chips each	4096 chips 128 µs	16 bits 64 µs	32 bits 128 µs

Fig. 1. TOA ranging and data waveforms. Our TOA ranging waveforms are derived from our CSMA-CA communications protocol.

The master radio initiates the TOA process and immediately performs an internal delay calibration, using the loop back through the pad shown in Fig. 2, to determine the master radio delay $(T_{\rm mt} + T_{\rm mr})$ for correction purposes. Ten trials are averaged to reduce the variance of the delay estimate. After calibration, the master radio transmits an RTS-T to the reference radio with a bit set in the TOA data field indicating the TOA ranging mode. The reference radio receives the RTS-T, reads the TOA data bit, performs an internal delay calibration to determine the reference radio delay $(T_{\rm rt} + T_{\rm rr})$, curve fits to refine the turnaround delay, and forms the TOA message. The TOA message can include GPS location data, results of the delay calibration, and turnaround delay refinement from curve fitting. The TOA message is transmitted back to the master that computes final one-way TOA, range, and relative position. The next $(M - 1)$ RTS-T/TOA-S message exchanges, if required, use different carrier frequencies and the shorter message, i.e., TOA-S, shown in Fig. 1. Delay calibrations and GPS data are not required due to the rapid rate at which these packets are exchanged.

The value for the master and reference radio antenna delay, i.e., Ta in Fig. 2, is a constant preloaded into the radios and combined with the results of delay calibration to reference the TOA to the antenna/air interface. We determine T_a by measuring the delay through a large sample of antennas and cabling over temperature and calculating the mean and standard deviation of the measured values.

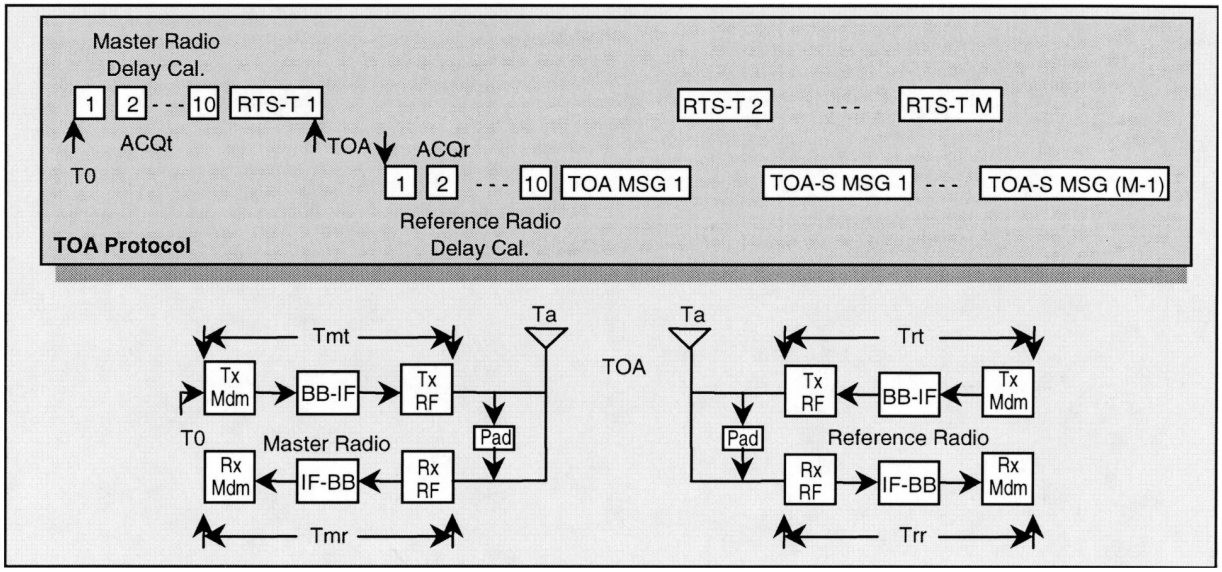

Fig. 2. TOA protocol timing. Integrating delay calibration into the TOA protocol is a key contributor toward meeting ±1-ns TOA accuracy.

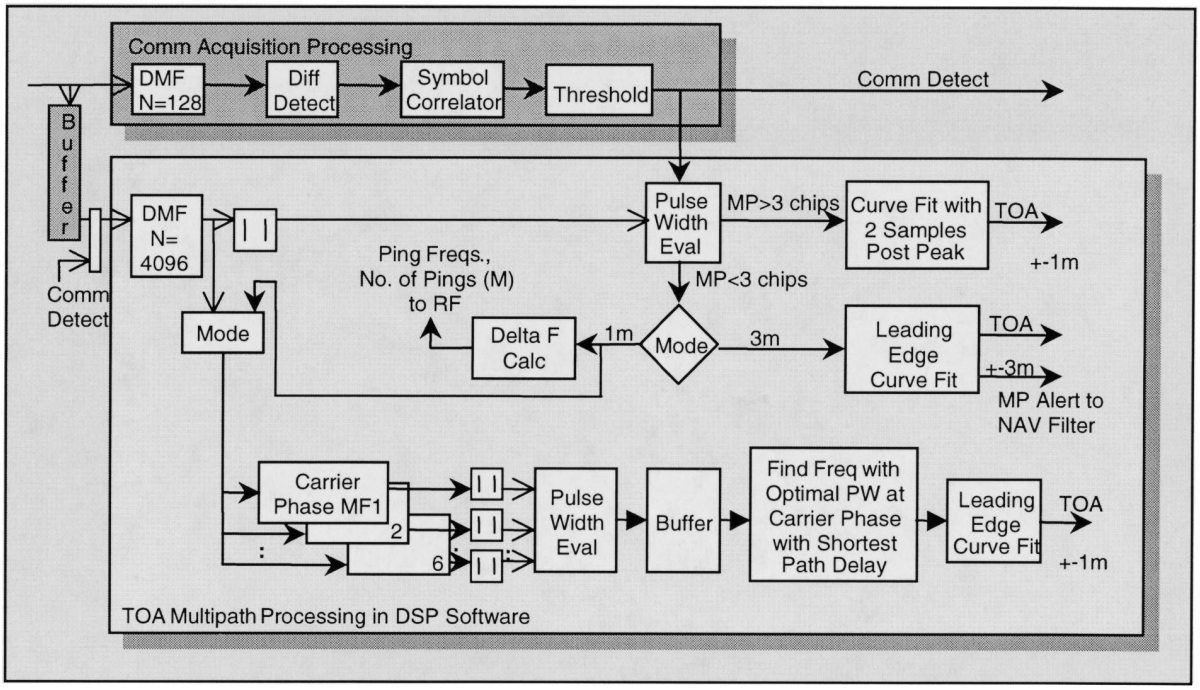

Fig. 3. TOA estimation. Using comm acquisition for initial TOA synchronization, digital-signal-processor throughput for refining the TOA estimate is reduced greatly.

C. TOA Estimation Algorithms

TOA processing takes advantage of the existing high-throughput communications acquisition processing hardware for triggering and an initial time mark. Shown in Fig. 3, our algorithm offers 1- and 3-m accuracy modes.

Upon communications acquisition pulse detection at the output of the symbol correlator, a pulse width discriminator at the output of the TOA synchronization digital matched filter (DMF) determines if the multipath is greater or less than three chips from the direct path. If the multipath is greater than three chips, the curve-fitting algorithm uses the leading edge samples

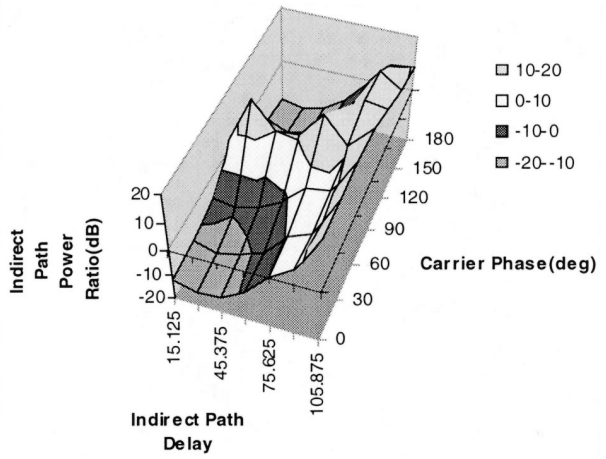

Fig. 4. Simulation results. TOA estimation accuracy is maintained at ± 1 ns for multipath stronger than direct path, and as close as 15 ns to the direct path.

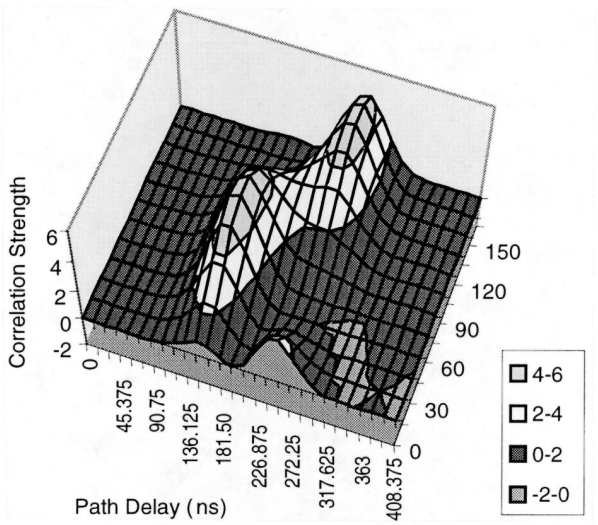

Fig. 5. Direct path–multipath orthogonality condition. Orthogonality separates multipath from direct path allowing curve fitting of the direct path without interference from multipath.

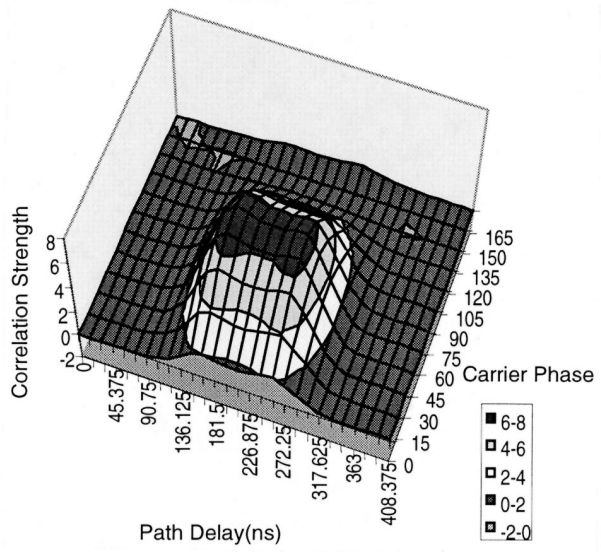

Fig. 6. Direct path–multipath in-phase condition. Multipath in-phase with the direct path smears the direct path, leading to an inaccurate curve fit.

plus two samples after the peak of the DMF response. Post peak samples can be used because multipath does not corrupt them in this case. If the multipath is less than three chips and 3-m accuracy is desired, a leading edge curve fit is implemented and a multipath alert is passed to the navigation filter that tracks the location solution. The filter determines the validity of the measurement and weights it accordingly. If the multipath is less than three chips and 1-m accuracy is desired, multiple pings at different carrier frequencies are required. Using the pulsewidth information, the system determines the number of pings and ping frequencies, and transfers control information to the RF subsystem of the radio.

Diverse frequencies create diverse carrier phases in multipath. Ranging performance is best when the carrier phase of the multipath is 90° with respect to the direct path. If this orthogonality condition is met, the direct path and multipath are separated and the direct path can be more precisely curve fitted with minimal effects from multipath. To determine the frequency of orthogonality, the in-phase and quadrature samples at the output of the TOA synchronization DMF rotate through carrier phase in 15° increments. A pulsewidth discriminator processes the data and buffers it until the M pings are completed. The data is searched to find the frequency where the optimal pulsewidth occurs at the carrier phase with the shortest path delay. This is the frequency where the direct path and multipath are orthogonal. The leading edge of the earliest pulse from the data at the frequency of orthogonality is curve fitted to determine the TOA estimate. In this case, i.e., 1-m accuracy with multipath present, the TOA subsystem performs multipath mitigation and the navigation filter uses the data directly without a weighting factor.

III. Performance

A. Cramer–Rao Bound of Performance

The lower bound on the rms error associated with a pair of radios is determined using the Cramer–Rao bound [6]

$$\mathrm{err}(i,j) = 1/\left[w(2bTR)^{1/2}\right] \tag{1}$$

where $R = (\mathrm{snr}_i \mathrm{snr}_j)^{1/2}/(1+\mathrm{snr}_i+\mathrm{snr}_j)^{1/2}$, $w = 2\pi f =$ rms spanned bandwidth, b is the signal bandwidth, and T is the coherent integration time. For our system, $f = b = 20$ MHz, $T = 128$ μs, and with $\mathrm{snr}_i = \mathrm{snr}_j = 4, R = 1.79$, resulting in a Cramer–Rao bound of $\mathrm{err}(i,j) = 0.08$ ns. Assuming that four TOA's are used to compute location in three dimensions, the total error is the root-sum-square of four components of error at 0.08 ns or $\mathrm{err}_{\mathrm{total}} = 0.16$ ns.

B. TOA Error Budget

The error budget results from adding the variances of the time delays of the radio components each time a TOA measurement signal passes through them. Total time delay t is a Gaussian random variable formed by summing a number of random variables or individual component time delays. A new random variable can be defined, i.e., d, such that $d = (1/M)\Sigma t_i\, i = 1, 2, \cdots, M$, where the variance of d is reduced by M, i.e., $\sigma_d^2 = \sigma_t^2/M$.

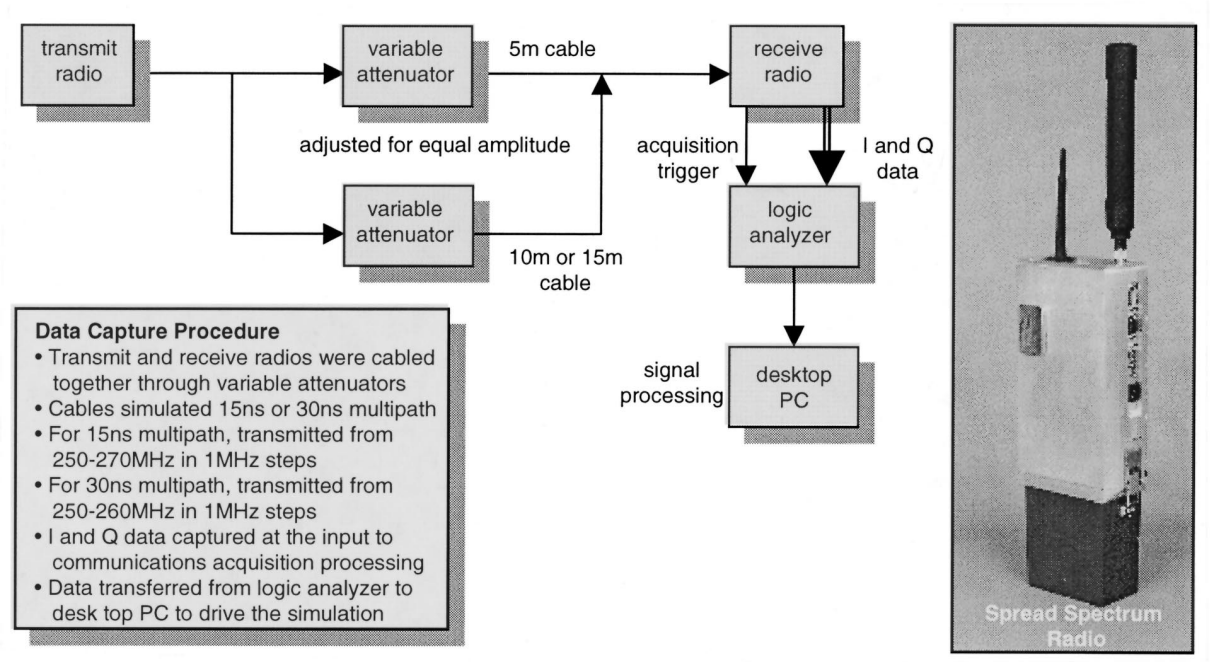

Fig. 7. Experimental setup. Our spread-spectrum radios were cabled together to capture multipath data for offline processing on the PC's.

To determine a single TOA, the system performs two delay calibrations (master and reference radios), sends two ranging messages (RTS-T, TOA message), and averages the results to determine the final TOA. The variance of the delay calibration error for the master radio is the sum of the variance of the delay in the transmitter and variance of the delay in the receiver. The reference radio contributes an equal amount. During transmission and reception of the RTS-T, the time-delay variance equals the sum of the variance of the master transmitter (including antenna) plus the variance of the reference receiver (including antenna). The TOA message is similar, except it is the sum of the reference transmitter delay variance and the master receiver delay variance. Since the TOA from the RTS-T and the TOA from the TOA message are averaged to determine the final TOA, the sum of the variances is reduced by a factor of 0.5. A maximum of eight RTS-T/TOA message exchanges are used at different carrier frequencies, but the two TOA's from one exchange are averaged to compute the final TOA solution. Writing the above in equation form serves as the TOA error budget as follows:

$$\sigma_{\mathrm{TOA}}^2 = 0.2\left(\sigma_T^2 + \sigma_R^2\right) + 0.5\left(\sigma_T^2 + \sigma_R^2 + 2\sigma_a^2\right). \quad (2)$$

The estimated TOA accuracy derives from the TOA error budget and by making several reasonable assumptions from experience. We found, to a good approximation, master and reference transmitter and receiver hardware achieves the same accuracy (see Fig. 2 for notation) as follows:

$$\sigma_{\mathrm{rf}} = \sigma_{\mathrm{bb-if}} = \sigma_{\mathrm{mdm}} = \pm 0.35 \text{ ns} \quad (3)$$

$$\sigma_T^2 = \sigma_{\mathrm{rf}}^2 + \sigma_{\mathrm{bb-if}}^2 + \sigma_{\mathrm{mdm}}^2 = 0.3675 \times 10^{-18} \quad (4)$$

$$\sigma_R^2 = \sigma_{\mathrm{rf}}^2 + \sigma_{\mathrm{bb-if}}^2 + \sigma_{\mathrm{mdm}}^2 + \sigma_{\mathrm{cf}}^2 = 0.3675 \times 10^{-18} + \sigma_{\mathrm{cf}}^2 \quad (5)$$

where $\sigma_{\mathrm{cf}}^2 = 0.25 \times 10^{-18} = \text{curve fit delay variance}$ as determined by simulation, and $\sigma_a^2 = 0.0625 \times 10^{-18} = \text{antenna delay variance}$ by assumption. Substituting the above into (2) yields

$$\sigma_{\mathrm{TOA}} = \pm 0.9 \text{ ns}. \quad (6)$$

C. Expected Performance in a Multipath Environment

We used simulation to estimate the performance of our TOA algorithm in a multipath environment. Our simulation generated a communications acquisition signal with an $\mathrm{SNR} = 6$ dB without the 4096-chip TOA synchronization sequence (this improvement will be added to the simulation in the near future). The multipath carrier phase varied from 0° to 180° with respect to the direct path while the multipath delay varied from 15 to 105 ns. We processed the signal through a software model of the communication acquisition processing and applied curve fitting. Fig. 4 illustrates multipath power causing 1-ns error in the leading edge curve-fitting algorithm. As shown, the value of multipath power causing an error of 1 ns, and peaks along the 90° carrier phase line. The results along the 90° line are summarized for convenience: (15.125 ns, 3 dB), (30.25 ns, 20 dB), (45.375 ns, 10 dB), (60.5 ns, 11 dB), 75.625 ns, 20 dB), (90.75 ns, 11 dB), and (105.875 ns, 20 dB). The variability in power ratio versus delay is caused by the correlation sidelobes of the pseudonoise (PN) sequence. The sidelobes will be lowered 15 dB with our new 4096-chip TOA synchronization sequence, and the corresponding results will be less variable. Fig. 5 shows how the correlation peaks separate when multipath is 90 ns from the direct path and 90° out of phase with the direct path. This allows curve fitting of the direct path without interference from the multipath, which degrades performance. Fig. 6 shows how the direct path and multipath correlation peaks combine to form a single broad peak when they are in phase. This condition leads to poor curve-fitting results.

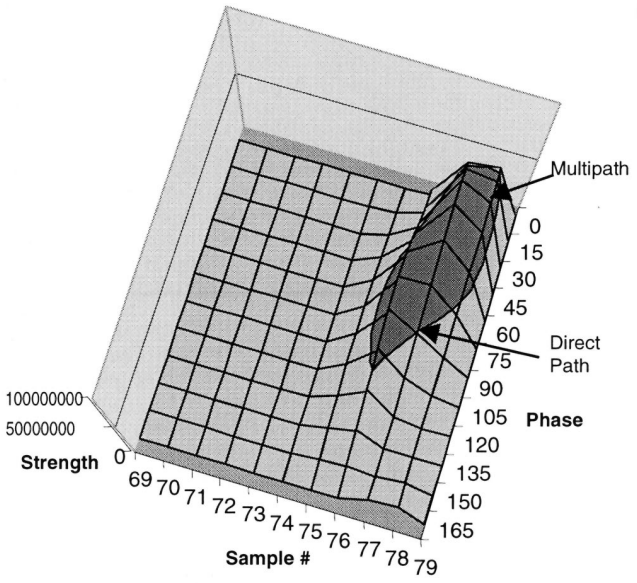

Fig. 8. Correlation versus carrier phase profile. Direct path and multipath separate at 90° for carrier frequency = 260 MHz and multipath delay by cable = 30 ns.

D. Experimental Results

Our experimental objectives were threefold as follows:

- demonstrate the occurrence of the direct path/multipath orthogonality condition within a 15-MHz change in carrier frequency for a multipath that is delayed by 15 ns from the direct path (equal amplitude), as expected from the relationship of the wavelength of the carrier frequency and the multipath delay;
- demonstrate the occurrence of the direct path/multipath orthogonality condition within an 8-MHz change in carrier frequency for a multipath that is delayed by 30 ns from the direct path (equal amplitude), as expected from the relationship of the wavelength of the carrier frequency and the multipath delay;
- show the potential for improvement in the curve-fit accuracy when the orthogonality condition occurs.

To meet the objectives, we chose to produce multipath in a controlled manner by using two different length cables to connect two radios together, one cable to emulate the direct path and one cable to emulate the multipath. The difference in the length of the cables provided the multipath delay of either 15 or 30 ns, as shown in Fig. 7.

For the 15-ns multipath case, we transmitted with a carrier frequency from 250 to 270 MHz in 1-MHz increments. For the 30-ns multipath case, we transmitted with a carrier frequency from 250 to 260 MHz in 1-MHz increments.

We captured data from the receiver of the reference radio in front of the traditional communications processing using a logic analyzer. We then transferred the data to a desktop personal computer (PC) where we performed the processing to find the orthogonality condition. We were not able to set up an accurate enough time reference with our test equipment to measure absolute TOA's to a meaningful accuracy, but we were able to demonstrate the orthogonality condition, the main objective of our experiment.

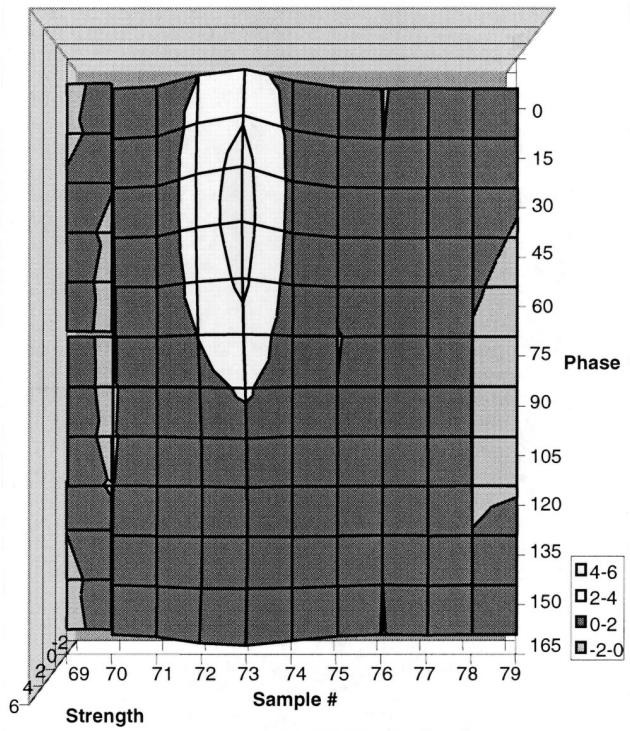

Fig. 9. Correlation versus carrier phase profile. Direct path and multipath smear at 0° for carrier frequency = 252 MHz and multipath delay by cable = 30 ns.

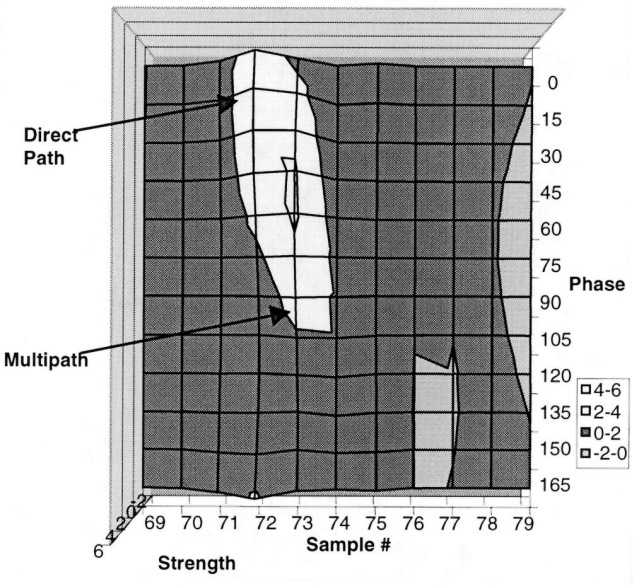

Fig. 10. Correlation versus carrier phase profile. Direct path and multipath separate at 90° for carrier frequency = 270 MHz and multipath delay by cable = 15 ns.

Figs. 8–11 show the results of processing the experimental data. Fig. 8 shows how the direct path and multipath separated at 90° for a carrier frequency of 260 MHz and 30 ns of delay between the direct path and multipath. Since the multipath is only 30 ns (one sample) from the direct path, the separation is not as pronounced as that shown in Fig. 5 where the separation is 90 ns (three samples) for illustration purposes. Curve fitting would be applied to the leading edge of the direct path. Fig. 9 shows the smearing of the direct path and multipath at 0° at a carrier frequency of 252 MHz for the 30-ns case as predicted,

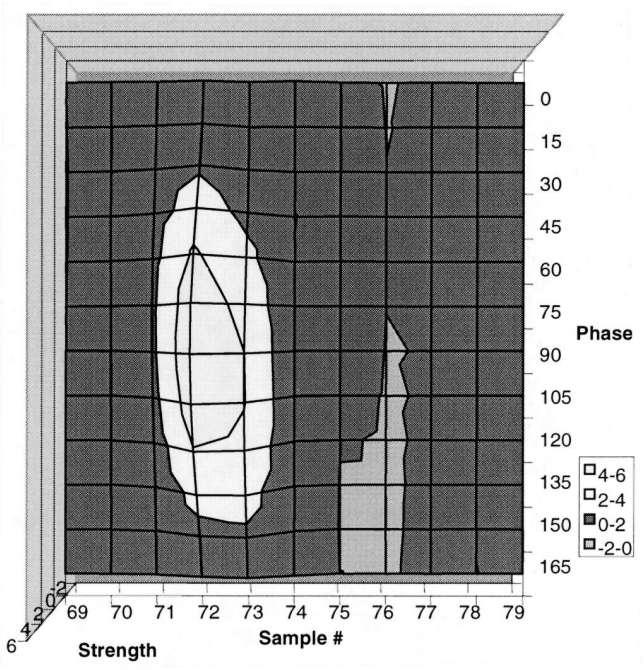

Fig. 11. Correlation versus carrier phase profile. Direct path and multipath smear at 0° for carrier frequency $= 255$ MHz and multipath delay by cable $= 15$ ns.

and curve fitting would yield inaccurate results. Figs. 10 and 11 exhibit similar behavior for the case where multipath is delayed by 15 ns from the direct path. Note that through symmetry we actually found -90° (in Fig. 10) for a carrier frequency of 270 MHz, but the separation of multipath from direct path still occurs and curve fitting would still be applied to the leading edge of the direct path. Fig. 11 shows the smearing of direct path and multipath at 0° for a 255-MHz carrier frequency, 15 MHz from the frequency at which orthogonality was found, as expected.

IV. Conclusion

Our two-way ranging technique combined with real-time system delay calibration will provide accurate ranging within the footprint of a handheld direct-sequence spread-spectrum DSSS radio without synchronizing target and reference radio clocks. The Cramer–Rao bound shows that sub-nanosecond accuracy is achievable in a nonmultipath environment. Using our diverse frequency ranging technique to orthogonalize the multipath and direct path, we can apply curve fitting to refine our TOA estimate while minimizing interference from multipath. This technique allows us to achieve TOA accuracies in severe multipath environments that are achievable in nonmultipath environments.

References

[1] T. S. Rappaport, J. H. Reed, and B. D. Woerner, "Position location using wireless communications on highways of the future," *IEEE Commun. Mag.*, pp. 33–41, Oct. 1996.

[2] K. Pahlavan, P. Krishnamurthy, and J. Beneat, "Wideband radio propagation modeling for indoor geolocation applications," *IEEE Commun. Mag.*, pp. 60–65, Apr. 1998.

[3] B. B. Peterson, C. Kmiecik, R. Hartnett, P. M. Thompson, and J. Mendoza, "Spread spectrum indoor geolocation," *Navigation*, pp. 97–102, Summer 1998.

[4] J. J. Caffery, Jr. and G. L. Stuber, "Overview of radiolocation in CDMA systems," *IEEE Commun. Mag.*, pp. 38–45, Apr. 1998.

[5] J. Werb and C. Lanzl, Designing a Positioning System for Finding Things and People Indoors.

[6] J. Werb and C. Lanzl, "The practical engineer: Designing a positioning system for finding things and people indoors," *IEEE Spectrum*, vol. 35, no. 9, pp. 71–78, Sept. 1998.

[7] S. Tekinay, E. Chao, and R. Richton, "Performance benchmarking for wireless location systems," *IEEE Commun. Mag.*, pp. 72–76, Apr. 1998.

Dennis D. McCrady (S'75–A'77–M'79–SM'82) received the B.S.E.E. degree from Purdue University, West Layfayette, IN, in 1970, and the M.S.E.E. and Ph.D.E.E. degrees from the University of Rhode Island, Kingston, in 1974 and 1980, respectively.

Since November, 1986, he has been with ITT Aerospace/Communications Division, ITT Industries, Clifton, NJ, where he is currently a Staff Scientist in secure information systems and has been involved with navigation, signal processing, and communications research and development. Most recently, he has been involved with developing spread-spectrum modems and integrating a TOA ranging capability within a spread-spectrum modem. Previously, he was the Lead System Engineer during the development of the GPS W-Sensor Program, in which ITT A/CD developed a nuclear detonation detection capability for Sandia National Laboratory and the U.S. Air Force. Prior to joining ITT A/CD, he was with the RCA Government Communications Division, Camden, NJ, AT&T Bell Laboratories, Holmdel, NJ, Raytheon Submarine Signal Division, Portsmouth, RI, and the Naval Underwater Systems Center, Newport, RI. He has authored or co–authored 14 papers. He holds one U.S. patent with two pending.

Lawrence Doyle received the B.S.C.S. degree from the Pratt Institute, Brooklyn, NY, and the M.S.C.S. degree from the Stevens Institute of Technology, Hoboken, NJ.

He has been with the Aerospace/Communications Division, ITT Industries, Clifton, NJ, for 14 years, and is currently a Staff Scientist in space systems software. He has been involved with software design for navigation and communications programs. Most recently, he has been involved with software design and TOA ranging. He was previously the Lead Software Engineer at ITT A/CD for the development of software for the GPS Total Navigation Payload for the U.S. Air Force.

Howard Forstrom received the B.E. and M.S.C.S. degrees from the Stevens Institute of Technology, Hoboken, NJ.

He has been with the Aerospace/Communications Division, ITT Industries, Clifton, NJ, for 12 years, and is currently a Senior Staff Engineer in space systems software. He has been involved with software design and project engineering for navigation and communications programs. Most recently, he has been involved with software design and TOA ranging. He was previously the Lead Software Engineer for the development of software for the GPS W-Sensor at ITT A/CD for Sandia Laboratories and the U.S. Air Force.

Timothy Dempsey received the B.S.E.E. degree from Santa Clara University, Santa Clara, CA, and the M.S.E.E. from Purdue University, West Layfayette, IN.

He has been with the Aerospace/Communications Division, ITT Industries, Clifton, NJ, for 14 years, and is currently a Systems Engineer specializing in wide-bandwidth radio development, statistical communication system analysis and modeling, and digital signal processing. Most recently, he has been involved with the design of the spread-spectrum modem at ITT A/CD. He previously contributed to the development of the spread-spectrum modem for ITT's Near Term Data Radio and to ITT's payload for the geostationing operational environmental satellite (GOES).

Marc Martorana received the B.S. degree in engineering science (with a mechanical concentration) from The College of New Jersey, Trenton.

He has been with the Aerospace/Communications Division, ITT Industries, Clifton, NJ, for four years, and is currently a Systems Engineer specializing in space and communication products. Most recently, he has been the Geolocation Integrated Product Team leader at ITT AC/D. He was previously involved in systems engineering for the GPS Total Navigation Payload and for the airborne version of ITT AC/Ds SINCGARS radio.